An investigative study of the interface heat transfer coefficient for FE modelling

An investigative study of the interface heat transfer coefficient for finite element modelling of high-speed machining

S A Iqbal*, P T Mativenga, and **M A Sheikh**
School of Mechanical, Aerospace, and Civil Engineering, University of Manchester, Manchester, UK

The manuscript was received on 25 March 2008 and was accepted after revision for publication on 23 June 2008.

DOI: 10.1243/09544054JEM1179

Abstract: This paper is concerned with the development of an experimental set-up and finite element (FE) modelling of dry sliding of metals to estimate the interface heat transfer coefficient. Heat transfer between the chip, the tool, and the environment during the metal-machining process has an impact on the temperatures and on the wear mechanisms, and hence on the tool life and on the accuracy of the machined component. For modelling of the metal-machining process, the interface heat transfer coefficient is an important input parameter to quantify the transfer of heat between the chip and the tool and to predict the temperature distribution accurately within the cutting tool. In previous studies involving FE analysis of the metal-machining process, the heat transfer coefficient has been assumed to be between 10 kW/m^2 °C and 100 000 kW/m^2 °C, with a background from metal-forming processes (especially forging). Based on the operating characteristics, metal-forming and metal-machining processes are different in nature. Hence there was a need to develop a procedure close to the metal-machining process, to estimate this parameter in order to increase the reliability of FE models. To this end, an experimental set-up was developed in which an uncoated cemented carbide pin was rubbed against a steel workpiece while the later was rotated at speeds similar to the cutting tests. This modified pin-on-disc set-up was equipped with temperature and force-monitoring equipment. An FE model was constructed for heat generation and frictional contact. The experimental and modelling results of the dry sliding process yield the interface heat transfer coefficient for a range of rubbing speeds.

Keywords: high-speed machining, frictional contact, interface heat transfer coefficient

1 INTRODUCTION

The work done to deform plastically and to shear away workpiece material during the machining process is largely converted into heat [**1**]. This heat energy increases the temperatures of the chip, the tool, and the machined surface. A very small amount of this heat energy is dissipated to the environment. The second-largest source of heat generation during the machining process for cases where the undeformed chip thickness is far greater than the tool edge radius has been identified as the frictional heat source in the secondary deformation zone. As a result, heat flows from the chip to the tool rake face and a thermal contact exists between these contacting surfaces. This heat transfer between the chip, the tool, and the environment has an impact on the temperatures and on the wear mechanisms, and hence on the tool life and on the accuracy of the machined surface. The heat transfer at the tool–workpiece interface is commonly assumed to be governed by the interface heat transfer coefficient. The interface heat transfer coefficient h can be defined by

$$h = \frac{q}{\Delta T} \tag{1}$$

where q is the average heat flow across the interface and ΔT is the temperature drop. It has been

*Corresponding author: School of Mechanical, Aerospace, and Civil Engineering, University of Manchester, A-29 Sackville Street, Manchester M60 1QD, UK. email: syed_a_iqbal@yahoo.com

established that the interface heat transfer coefficient is a function of several parameters, the dominant parameters being the contact pressure, the interstitial materials, the macrogeometry and microgeometry of the contacting surfaces, the temperature, and the type of lubricant or containment and its thickness [**2**].

For the finite element (FE) modelling of metal-machining processes, the boundary conditions at the tool–chip interface are usually formulated in terms of the interface heat transfer coefficient. Thus, the interface heat transfer coefficient is an important input parameter to quantify the transfer of heat between the chip and the tool, and to predict the temperature distribution accurately within the cutting tool. In all the previous work on FE modelling of the metal-machining process, the numerical values used for defining the interface thermal boundary condition were taken from metal-forming processes (mostly metal forging). A discussion is presented in this paper regarding the differences in the nature and operating characteristics of machining and forging processes. It is concluded from this discussion that there is a need to develop a procedure close to the metal-machining process, to estimate this parameter in order to increase the reliability of FE models. Because of experimental difficulties in measuring the temperature at the tool–chip interface, a new method for estimating values of the interface heat transfer coefficient is presented. It is based on a simplified set-up of two-body heat transfer with the amount of heat generated in the rubbing process depending on the rotational speed. The interface heat transfer coefficient for this sliding contact scenario is predicted by using the FE modelling approach.

2 EXISTING SCENARIO FOR INTERFACE HEAT TRANSFER COEFFICIENT VALUES IN MACHINING SIMULATIONS

In the application of the interface heat transfer coefficient to the chip formation simulations, very high values of h have been used on the assumption of perfect contact. Yen *et al.* [**3**] used a very high value (value not mentioned) of the interface heat transfer coefficient to study the effect of the tool geometry on the orthogonal machining process, assuming perfect contact between the chip and the tool. In another study, Yen *et al.* [**4**] again used a very high value of interface heat transfer coefficient (value not reported) to model tool wear in orthogonal machining, again for perfect contact. To simulate the orthogonal machining process employing coated tools, again assuming perfect thermal contact between the tool and the chip, Yen *et al.* [**5**] used a value of 100 kW/m^2 °C for the interface heat transfer coefficient. The workpiece material used was AISI 1045 steel with a tungsten carbide tool, coated with different coatings at a cutting speed of 220 m/min. Klocke *et al.* [**6**] also assumed a very high value of the interface heat transfer coefficient between the tool and the chip for the orthogonal machining of AISI 1045 steel with a ceramic tool at ultra-high cutting speed. Their assumption was based on experimental results for the temperature and chip surface in the secondary deformation zone.

Marusich and Ortiz [**7**] used the first law of thermodynamics to account for the thermal effects produced during the cutting process. The heat generated at the sliding contact was considered to be a function of the difference in the velocity across the contact. This was divided proportionately between the tool and the chip based on their thermal conductivity, density, and heat capacity values. Ozel [**8**] used a value of 100 kW/m^2 °C as the interface heat transfer coefficient to study the effect of different friction models on the output of an orthogonal machining process on low-carbon resulphurized free-cutting steel (LCFCS). Xie *et al.* [**9**] simulated two-dimensional tool wear in the turning of AISI 1045 steel with an uncoated tungsten carbide tool at a cutting speed of 300 m/min. Their FE model used a value of 10 kW/m^2 °C to define the gap conductance at the tool–chip interface. Miguélez *et al.* [**10**] simulated the orthogonal metal-cutting process by using two different numerical approaches, i.e. Lagrangian and arbitrary Lagrangian Eulerian, with different chip separation criteria. Here, the relation defining the heat flux crossing the tool–chip interface was directly related to the interface gap conductance. The value of gap conductance was again assumed to be very high for perfect heat transfer between the tool and the chip. Coelho *et al.* [**11**] simulated the orthogonal metal-cutting process using the arbitrary Lagrangian Eulerian approach for an AISI 4340 steel as the workpiece and Polycrystalline cubic boron nitride (PCBN) as the cutting tool using finishing cutting parameters. A gap conductance value of 500 kW/m^2 °C was used considering perfect heat transfer. Arrazola *et al.* [**12**] simulated the orthogonal metal-cutting process for the study of serrated chip formation during simulation of the metal-cutting process using the arbitrary Lagrangian Eulerian approach. They analysed the sensitivity of serrated chip prediction to the numerical and cutting parameters using AISI 4140 steel as the workpiece and uncoated ISO P10 grade carbide as the cutting tool. A gap conductance value of 10^5 kW/m^2 °C was used considering heat transfer with perfect thermal contact. Table 1 summarizes the values of the interface heat transfer coefficients used for simulation of the metal-machining process.

Table 1 Summary of the interface heat transfer coefficient values used for machining simulation

Reference	Workpiece material	Tool material	h(kW/m^2 °C)
Yen *et al.* [**3**]	AISI 1020	Uncoated WC	*
Yen *et al.* [**4**]	AISI 1045	TiC/Al_2O_3/TiN coated WC	100
Yen *et al.* [**5**]	AISI 1045	Uncoated WC	100
Klocke *et al.* [**6**]	AISI 1045	SiC–Ceramic	*
Ozel [**8**]	LCFCS	Uncoated WC	100
Xie *et al.* [**9**]	AISI 1045	Uncoated WC	10
Miguélez *et al.* [**10**]	42CrMo4	Uncoated WC	*
Coelho *et al.* [**11**]	AISI 4340	PCBN	500
Arrazola *et al.* [**12**]	AISI 4140	ISO P10 carbide	100 000

* Value not reported. Perfect contact was assumed between tool and workpiece.

3 METHODS USED PREVIOUSLY FOR THE ESTIMATION OF THE INTERFACE HEAT TRANSFER COEFFICIENT

Many different approaches have been used to estimate the interface heat transfer coefficient. However, most of the previous work focused on hot- and cold-forming processes rather than machining. For these (forming) processes, analytical, experimental, and numerical approaches were used to define and estimate heat transfer between solids under sliding contact. Most of the analytical studies estimated the contact temperature by considering two semi-infinite solids under steady state conditions and assuming a band, circular, or elliptically shaped contact, with applications in strip rolling [**13**–**16**]. Bos and Moes [**17**] used asymptotic solutions for circular and semi-elliptic band contact to analyse the heat partitioning problem by matching surface temperatures. Their solutions covered a wide range of Peclet numbers. Bauzin and Laraqi [**18**] used the least-squares method to estimate the heat generated, thermal contact conductance, and heat partition coefficient simultaneously.

The experimental work has mainly focused on the determination of heat partition and thermal contact conductance. Berry and Barber [**19**] developed a symmetric cylinder-on-cylinder experimental set-up to study the division of frictional heat in sliding contact. They concluded that oxide films have an appreciable effect on the microscopic thermal resistance. Lestyan *et al.* [**20**] developed a test rig to perform dry sliding of a alumina–steel pair to analyse contact and temperatures developed in the contact region. Some experimental studies for determining the thermal contact conductance were conducted using devices which contained two tools or two tools with a workpiece sandwiched between them [**21**–**24**]. These experiments were followed by an assessment of the interface heat transfer coefficient whilst the specimen deformed plastically.

Another method was based on the solution of an inverse problem; a sequential inverse method was used to determine the thermal contact conductance in metal-forming processes [**25**]. A further method was based on matching the experimentally measured temperature with analytical and/or numerical solutions for various values of h. The interface heat transfer coefficient was taken to be the value which provided the best match between simulation and experimental results [**23**, **24**, **26**].

4 EFFECT OF OPERATING PARAMETERS ON THE h VALUE IN FORGING PROCESSES

As mentioned earlier, the interface heat transfer coefficient is influenced by several operating parameters such as the pressure, the macrogeometry and microgeometry of the contacting surfaces, and the temperature. In this section, the effects of these operating parameters on the interface heat transfer coefficient are discussed.

4.1 Effect of the pressure

During the forging process, the pressure applied by closing the die largely influences the interface heat transfer coefficient. Semiatin *et al.* [**21**] reported an experimental and analytical technique for the determination of the interface heat transfer coefficient for non-isothermal bulk forming process. Two instrumented dies were heated to different temperatures and brought together under various pressure levels. A one-dimensional analysis and a finite difference model were used in the evaluation of the interface heat transfer coefficient. They concluded that, in the absence of deformation, the heat transfer coefficient increases with increasing interface pressure. Above a threshold pressure, the interface heat transfer coefficient becomes insensitive to the forging pressure. Similar results were reported by Lambert *et al.* [**27**] and Lambert and Fletcher [**28**]. They produced design graphs for the thermal contact conductance for three major aerospace alloys, with a pressure up to 100 MPa and a temperature of 300 K. Hu *et al.* [**29**] also reported a similar trend of increase in the heat transfer coefficient with increasing interface

pressure, for the forging of Ti–6A–l4V alloy. The temperature and pressure taken in their study were 920 ^{o}C and 500 MPa respectively.

4.2 Effect of the temperature

Malinowski *et al.* [**22**] studied the heat transfer coefficient as a function of the temperature and pressure. They used temperature measurement in two dies in contact and employed the FE method to determine the interface heat transfer coefficient. They developed an empirical relationship, giving the interface heat transfer coefficient as a function of the time, temperature and interfacial pressure. However, they neglected the heat generation within the workpiece. They concluded that the interface heat transfer coefficient was not as strongly dependent on the temperature as it was on the pressure.

4.3 Effect of interface friction

Burte *et al.* [**24**] studied the coupling between the heat transfer coefficient and friction during the hot-forging process. They analysed the data from ring compression tests combined with generation of the heat transfer coefficient and friction shear factor calibration curves derived from FE simulations. They reported that the effect of the friction shear factor on the heat transfer coefficient was small. Their simulation results and corroborating experimental observations led to the conjecture that heat transfer and friction may be decoupled in the analysis of the metal-working process for similar geometry and processing conditions.

4.4 Effect of the deformation speed

Semiatin *et al.* [**21**] deduced from a ring compression test, involving both deformation and heat transfer, that the heat transfer coefficient increased with increasing deformation rate. A similar trend was also reported by Hu *et al.* [**29**], with strain rates of $0.125\,s^{-1}$ and $1.0\,s^{-1}$ and with higher values of pressure and temperature in comparison with those to one used by Semiatin *et al.* [**21**]. This can be explained by the fact that, at high deformation rates, most of heat transfer occurs simultaneously with the process which tends to smooth interface asperities. On the contrary, at low deformation rates, heat transfer occurs prior to large deformation.

4.5 Effect of the surface roughness

Lambert and Fletcher [**28**] studied the effect of a non-flat, rough, and metallic coated surface on the thermal contact conductance. They concluded that the interface heat transfer coefficient increased with increasing roughness of the contacting surfaces. Rough surfaces add more resistance to the transfer of heat. Similarly, in the case of lubricants and coatings applied to the interface during forging process to reduce interfacial friction, this also adds to the resistance to heat transfer between contacting surfaces, thereby resulting in a reduction in the interface heat transfer coefficient.

5 COMPARISON BETWEEN THE MACHINING AND FORGING PROCESSES: OPERATING CHARACTERISTICS

Based on the discussion presented earlier, there are some contrasting factors related to the nature of bulk forming and machining. In the case of the hot-bulk-forming process, the interface heat transfer coefficient is influenced by the rate of deformation encountered during the process. The maximum strain rates involved in forging processes are of the order of $10^3\,s^{-1}$ [**30**] and are relatively low compared with those in the machining process. The deformation rates involved during the machining processes, on the other hand, are very high, typically of the order of $10^6\,s^{-1}$ [**31**]. Similarly the difference in temperatures involved in these processes is very high. Kalpakjian [**30**] reported that the homologous temperature (ratio of operating temperature to the melt temperature) for forging processes ranges between 16 per cent and 70 per cent, whereas for machining processes it can be up to 90 per cent, i.e. closer to the melt temperature and higher compared with forging processes.

The contact area is also a critical issue in this comparison, as it provides a passage for heat transfer between mating surfaces. In the case of metal machining, the contact area between the tool and the chip is small and does not vary substantially during the machining process. In the machining of AISI 1045 steel with uncoated cemented carbide, the contact area decreases with increasing cutting speed for cutting speeds up to 900 m/min [**32**]. However, in the case of metal forging (considering the case of upset forging), the contact area increases substantially with increasing percentage reduction in height during the forming process. Also, the natures of contact in the two processes under consideration are different. In the case of forging, mating components remain in contact during the whole process whereas, in the case of machining, fresh workpiece material comes in contact continuously with the tool rake face. For the latter case, it is necessary to develop an experimental set-up for the determination of the interface heat transfer coefficient suitable for the machining process.

6 RUBBING EXPERIMENTS

An experimental set-up adapted from that proposed by Lancaster [**33**] and Olsson *et al.* [**34**], for the study of wear was used in this case to study the heat transfer problem. Rubbing tests were performed, where the end surface of a cylindrical pin made of tool material was pressed against the end surface of a rotating workpiece. For these tests, a pin of 2.5 mm diameter and 15 mm length was made of cemented tungsten carbide (same grade as ISO P10–P20 cutting tool). The end surface of the pin was ground to a negative relief angle (approximately 5–10°) so as to avoid chip formation. The mass of the pin was measured using a precision electronic balance to calculate the amount of mass loss during the rubbing process. The pin was assembled on the tool holder in order to regulate its radial position compared to the thickness of the cylindrical workpiece. The tool holder was then mounted on a Kistler three-component piezoelectric dynamometer to measure the forces. An AISI 1045 workpiece of a hollow cylindrical shape with a wall thickness of 2.5 mm was used. The rubbing experiments were performed at the rubbing speeds of 56, 139, 195, 279, 391, 441, 558, and 776 m/min, on a lathe machine equipped with an infrared thermal imaging camera and a force dynamometer. The rubbing time was set to 1 min for all rotational speeds in order to achieve a steady state temperature in the pin and the experiments were repeated three times. The experimental set-up is shown in Figs 1 and 2.

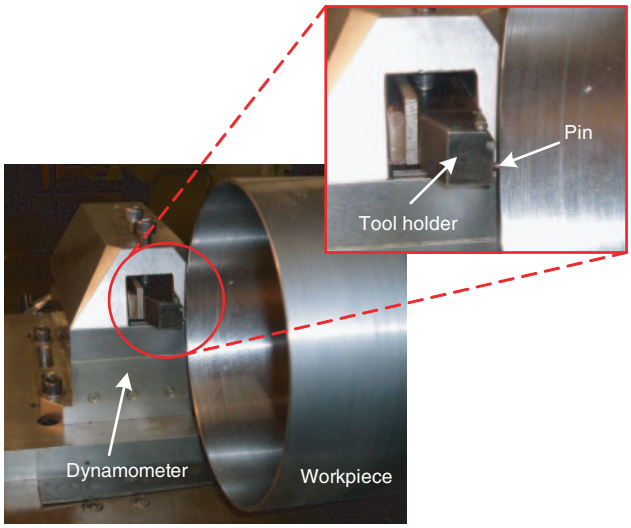

Fig. 1 Experimental set-up for the pin-rubbing tests

The temperatures were measured using an infrared thermal imager FLIR ThermalCAM_SC3000. This system is a long-wave and self-cooling analysis system with a cool-down time of less than 6 min. The accompanying software package allows detailed analysis of highly dynamic objects and events typically found in metal-machining applications. The thermal imaging camera has a temperature range from 20 °C to 2000 °C with an accuracy of ±2 °C for the measurement range above 150 °C. This camera can capture and store thermal images and data at high rates (up to 750 Hz for PAL and 900 Hz for NTSC format) with the ThermaCAM Researcher™ 2.8 package.

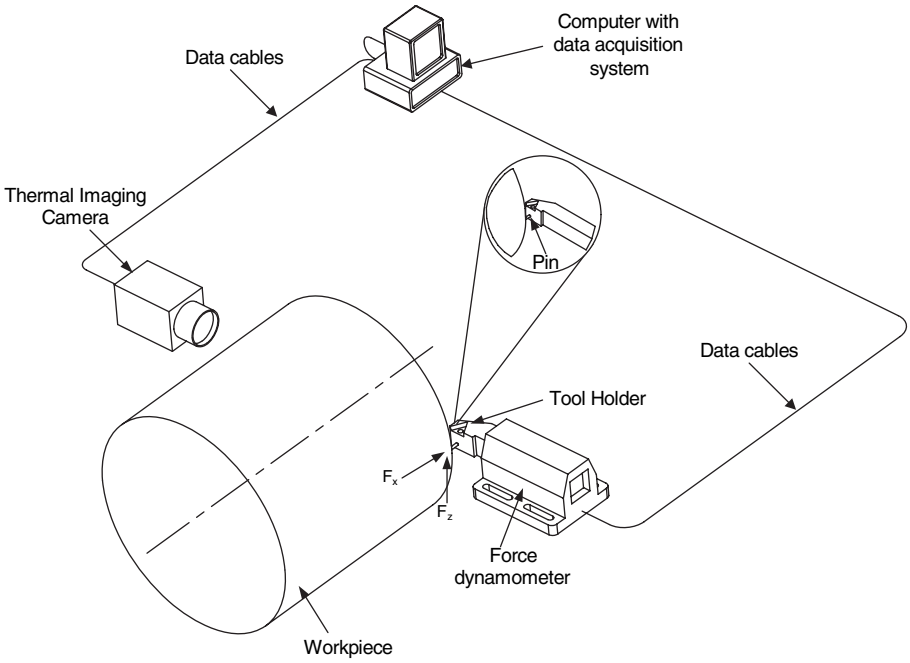

Fig. 2 Schematic representation of the experimental set-up for the pin-rubbing test (showing the position of the thermal imaging camera)

Table 2 Technical specifications of the FLIR system infrared thermal imaging camera

Infrared detector	Quantum well infrared photodetector
Spectral range	8–9 μm
Image frequency	50–60 Hz non-interlaced (standard), up to 750–900 Hz (optional and with Researcher HS option)
Thermal sensitivity	20 mK at 30 °C
Temperature range	–20 °C to +2000 °C
Accuracy	±1 °C (for measurement ranges up to +150 °C) ±2 °C (for measurement ranges above +150 °C)
Spatial resolution	1.1 mrad
Pixel per image	320 × 240
Zoom factor	4 ×
File format	14-bit radiometric infrared digital image (*.IMG), 8-bit standard bitmap (*.BMP)

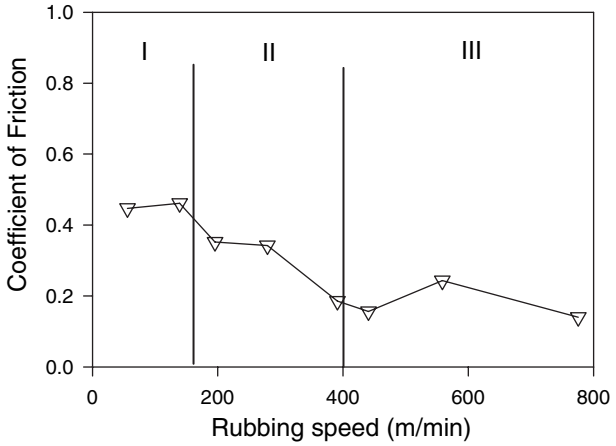

Fig. 3 Variation in the coefficient of friction with the rubbing speed

Complete technical specifications of the thermal imaging system are given in Table 2.

Figure 2 shows the position of thermal imaging camera in the experimental set-up. The camera was positioned at a distance of 45 cm from the pin. The stored images were recalled and analysed by using the available software. When placed on the image the cursor gave the temperature value at the required points. For the rubbing time specified, the pin acquired a uniform temperature in the portion extended from the holder. The real temperature of an object depends strongly on the emissivity of the material, which is of particular concern when a thermal imaging camera is used. An accurate calibration of the thermographic system was carried out to find the emissivity value of the rubbing pin material (ISO P20 grade uncoated cemented carbide). Samples were heated to temperatures ranging from 100 °C to 900 °C in an oven. A thermocouple–infrared pyrometer arrangement was used to read the temperature of the pin, and the emissivity adjusted until the temperature reading of the pyrometer matched a thermocouple reading. The average thermal emissivity of the uncoated cemented carbide pin was found to be 0.55 at 700 °C.

7 EXPERIMENTAL RESULTS AND DISCUSSION

The experimental results are presented in Figs 3, 5, and 7. Each data point on these graphs was calculated from measurement of three rubbing tests, shown with corresponding variation in data. Figure 3 shows the variation in the coefficient of friction with the rubbing speed. This was calculated from the forces measured during the rubbing process. It shows an overall decreasing trend with increasing rotating speed, similar to the results of other cutting experiments [**32**, **35**]. However, the numerical values of the friction coefficient obtained from these rubbing tests are lower than the previously reported values of cutting experiments for a similar range of speeds [**32**, **35**]. This could be explained by the absence of any sticking in the rubbing tests as compared with the cutting experiments.

Figure 4 shows the variation in the maximum temperature measured at a specified location on the pin, with respect to time. Initially there are a few spikes of high temperature (due to the chip formation) but soon afterwards the temperature becomes steady.

Figure 5 shows the variation in the pin temperature with the rubbing speed. The pin temperature rises sharply in the speed range 195–558 m/min but then stabilizes after that speed in the temperature range 700–900 °C. This can be explained in the context of the variation of thermal conductivity of uncoated cemented tungsten carbide. Childs *et al.* [**36**] reported that the thermal conductivity of ISO P grade uncoated cemented tungsten carbide decreases with increasing temperature (Fig. 6). This can account for the flatter slope of pin temperature curve at high speeds.

The variation in the pin wear with the rubbing speed is shown in Fig. 7. Initially the pin material

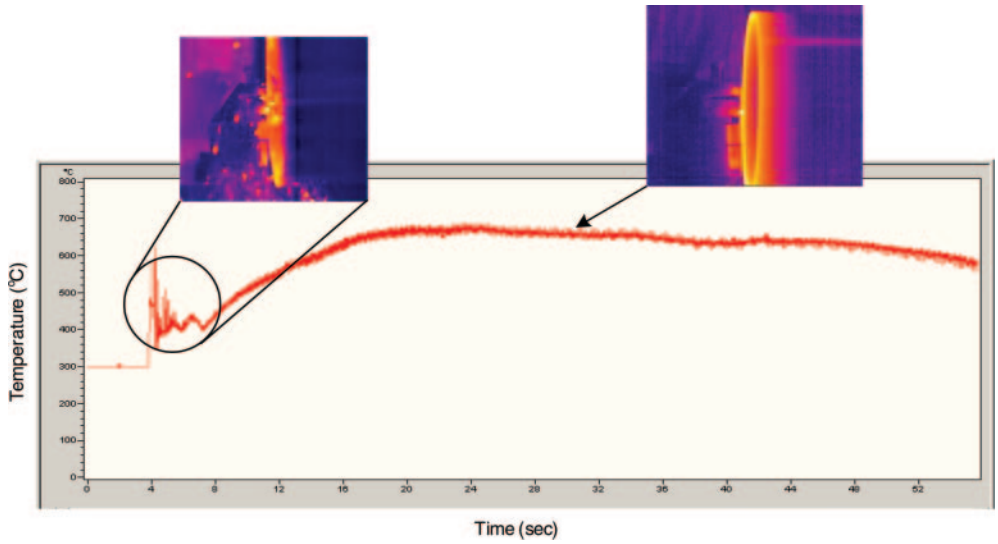

Fig. 4 Maximum pin temperature measured during the rubbing process, using the thermal imaging camera

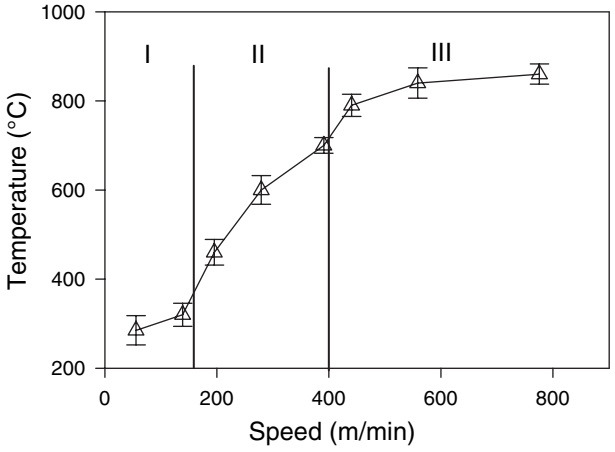

Fig. 5 Variation in the pin temperature with the rubbing speed

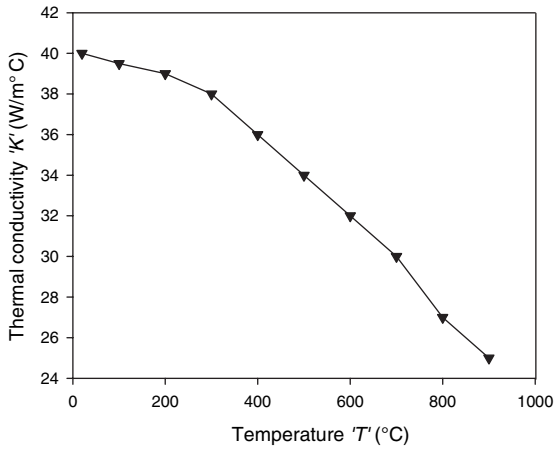

Fig. 6 Variation in the thermal conductivity with the temperature for P20 carbide [**36**]

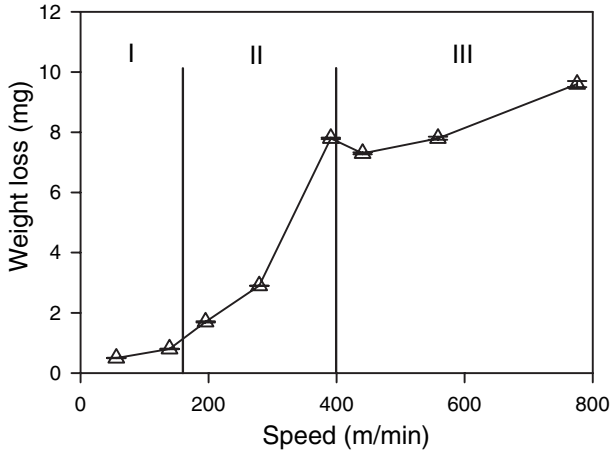

Fig. 7 Variation in the mass loss of the pin with the rubbing speed

loss is low up to a rubbing speed of 279 m/min but it rises sharply at a rubbing speed of 391 m/min. It then drops slightly at a rubbing speed of 441 m/min but increases again at a steady rate. It should be noted that the variations in the pin temperature and pin mass loss with rubbing speed follow a similar trend. Figure 8 shows that the pressure is approximately constant for all the rubbing speeds, except for the lowest speed.

It is evident from the results presented in Figs 3, 5, and 7 that there is a marked transition in their behaviour. There are three regions which can be identified for all three variables: region I, for speeds less than 200 m/min; region II, for speeds greater than 200 m/min and less than 600 m/min; region III, for speeds greater than 600 m/min. For rubbing speeds less than and equal to 200 m/min (region I), the loss of pin mass is negligible. For the rubbing speed interval 200–600 m/min, the loss of pin mass

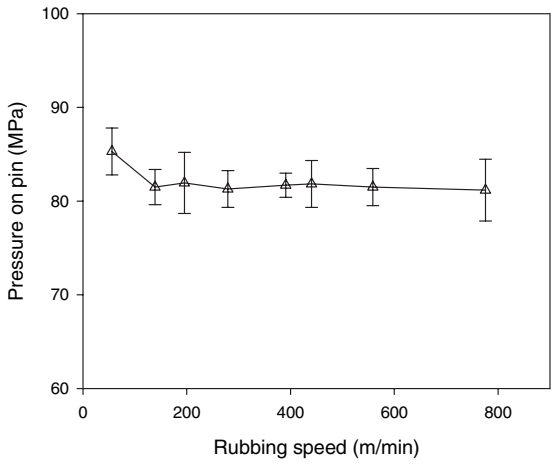

Fig. 8 Variation in the pressure applied on the pin at different rubbing speeds

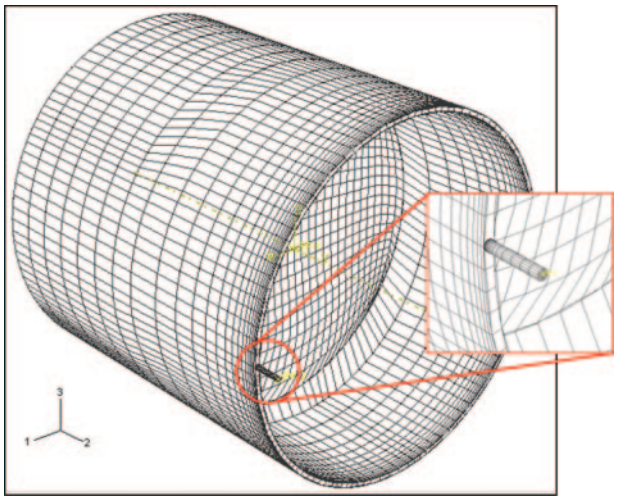

Fig. 9 FE model of the rubbing process

is very high. Similarly the temperature rises sharply in regions I and II but stabilizes in region III. Correspondingly the coefficient of friction decreases in these two regions, i.e. in regions I and II, and stabilizes in region III.

In the next section an FE model of the pin rubbing set-up will be discussed. The scheme followed is to vary the interface gap conductance to match the experimental pin temperature.

8 FE MODELLING

In order to simulate the rubbing process numerically, a commercial FE package ABAQUS/Explicit was used. An FE model was developed and the simulations were run with conditions similar to the experiments. As the problem involved a number of strongly interacting mechanical and thermal processes such as friction, temperature, and wear, a coupled thermomechanical model was developed. The heat produced by friction (mechanical work) acts as a source for the thermal problem. The work presented here is based on the rubbing process only, i.e. wear is neglected. This is justifiable because the volume of material removed (in milligrams) from the pin during the rubbing process was very low compared with that from the advanced wear processes involved in real machining. The FE model used for simulating the rubbing process is shown in Fig. 9. In this model, the carbide pin was held stationary, while the AISI 1045 steel workpiece revolves with a rubbing speed ranging from 56 m/min to 776 m/min. A graded mesh was used for both the pin and the workpiece, with higher mesh density in the interface zone.

With reference to Fig. 9, the boundary conditions used for the model are defined as follows: the contact surfaces of the pin and the workpiece were assumed to be smooth and in perfect contact. The contact between the pin and workpiece was evaluated by using an optical microscope to examine the pin face. The wear marking on the pin showed full contact. The exterior boundaries are exposed to still air except for the contacting regions of the pin and the workpiece. For exterior regions, the convective heat transfer coefficient is assumed to be $h_\infty = 0.02\,\mathrm{kW/m^2\,^\circ C}$ [**37**]. Any heat loss due to radiation is neglected. The whole model was set at room temperature. The experimental values of coefficient of friction (shown in Fig. 3) are used at the interface of the pin and the counter material for each rubbing speed. The material properties used for the pin and the workpiece materials are listed in Tables 3 and 4 respectively.

In the application of contact formulation for FE model, the carbide pin is taken as the 'slave' and the AISI 1045 steel workpiece as the 'master'. Heat partition is an important issue in sliding contact of two bodies for which several approaches have been followed by different researchers [**7**, **38**, **39**]. For the FE model developed for this study, the heat partition ratio at the interface between the pin and the workpiece is given mathematically by

$$\frac{H_1}{H_2} = \frac{\sqrt{\rho_1 K_1 C_1}}{\sqrt{\rho_2 K_2 C_2}} \tag{2}$$

where H is the heat partition, ρ is the density ($\mathrm{kg/m^3}$), K is the thermal conductivity ($\mathrm{W/m^2\,^\circ C}$), and C is the specific heat capacity ($\mathrm{J/m^2\,^\circ C}$). The subscripts 1 and 2 represent the pin and workpiece materials respectively. Temperature-dependent data, given in Table 3, was used to evaluate equation (2).

The interface heat transfer coefficient between the pin and the workpiece is defined in the FE model

Table 3 Thermal and mechanical properties of the pin [**37**] (pin material, uncoated cemented carbide*)

	Thermal expansion		Heat capacity		Modulus of elasticity		Thermal conductivity	
Poisson's ratio	Value ($\times 10^{-6}\,^{\circ}C^{-1}$)	Temperature (°C)	Value ($J/mm^3\,^{\circ}C$)	Temperature (°C)	Value (Gpa)	Temperature (°C)	Value (W/m°C)	Temperature (°C)
0.22	6.3	20–800	3.66	240	520	20	40	20
			3.8	450	509	200	39.5	100
			4.31	640	494	300	39	200
			5.1	695	487	500	38	300
					487	700	36	400
							34	500
							32	600
							30	700
							27	800
							25	900

* Room temperature properties were provided by Sandvik Coromant. For the temperature-dependent properties, data from reference [**36**] is followed.

Table 4 Thermal and mechanical properties of the counter material [**37**] (workpiece, AISI 1045)

	Thermal expansion		Heat capacity		Modulus of elasticity		Thermal conductivity	
Poisson's ratio	Value ($\times 10^{-05}\,^{\circ}C^{-1}$)	Temperature (°C)	Value ($J/mm^3\,^{\circ}C$)	Temperature (°C)	Value (Gpa)	Temperature (°C)	Value (W/m°C)	Temperature (°C)
0.3	1.12	100	3.66	25	215	20	45	25
	1.19	200	3.8	125	210	200	42.5	100
	1.27	300	4.31	325	165	400	38	300
	1.35	400	5.1	525	160	600	34.5	500
	1.41	500	8.76	725			29	700
	1.45	600	8.27	825			28	800
	1.46	700	7.48	875			24	900
			6.04	925			23	950
			5.64	975			23	1000
							24	1050
							26	1100
							27	1150

by the gap conductance. This parameter controls the amount of heat flowing through the interface. The strategy used here was to vary the value of the gap conductance in the simulation and to match the simulated temperatures on the pin with experimental values at the same location. For the matched temperatures, the gap conductance value used in the simulation defined the interface heat transfer coefficient. During the rubbing experiments, only a small length of the pin protruded from the tool holder in order to avoid any excessive pin deflection or breakage. Owing to this short protruded length of the pin, the measured temperature of the pin was almost uniform.

9 NUMERICAL RESULTS

A series of simulations for all the rubbing speeds ranging from 56 m/min to 776 m/min were carried out. The interface heat transfer coefficient values for these speeds, following the procedure outlined in the previous section, are shown in Fig. 10. These results show that the value of interface heat transfer coefficient is initially high ($300\,kW/m^2\,^{\circ}C$) for a low rubbing speed of 56 m/min. The value then reduces to $100\,kW/m^2\,^{\circ}C$ at 139 m/min and remains constant until the rubbing speed of 279 m/min. After that, it increases to a value of $150\,kW/m^2\,^{\circ}C$ for the rubbing speed of 441 m/min and again decreases to a value of $100\,kW/m^2\,^{\circ}C$ at 776 m/min. By examining the pin temperatures for this speed range (Fig. 5), the pin temperature rises steadily before stabilizing for high rubbing speeds (greater than 558 m/min). The pin wear rate shows a direct dependence on the pin temperature (Fig. 5). As shown in Fig. 8, the pressure corresponding to the load applied on the pin approximately remains constant except for the very low speed. In this context, by comparing Fig. 5 and Fig. 10, it is observed that the interface heat transfer coefficient initially shows a decreasing trend with increasing temperature (for the two lowest rubbing

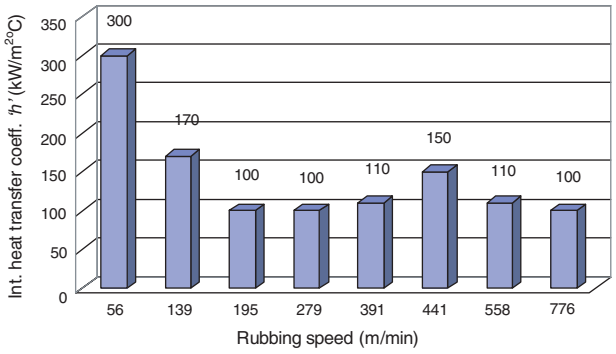

Fig. 10 Variation in the interface heat transfer heat coefficient with the rubbing speed

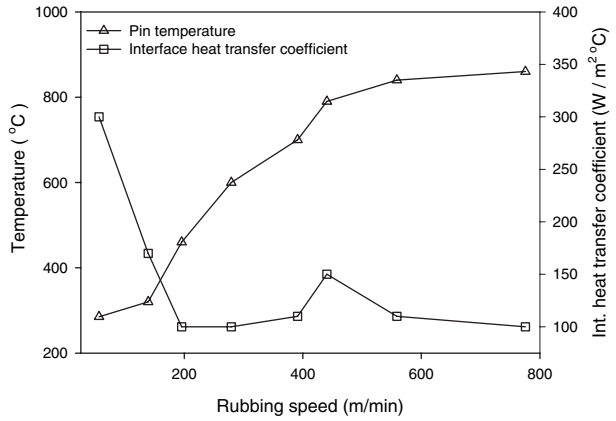

Fig. 11 Variation in the pin temperature and interface heat transfer coefficient with the rubbing speed

speeds) and afterwards it becomes constant for high rubbing speeds. Thus the interface heat transfer coefficient shows a dependence on the temperature for low rubbing speeds (Fig. 11).

For the forging methods, the temperature of both the workpiece and the die are varied for the estimation of interface heat transfer coefficient. Also, heat generated during bulk forming is involved in the process. For the rubbing process on the other hand, both the pin and the workpiece are at the surrounding temperature and the source of heat generation is rubbing and sliding only. As mentioned earlier, Malinowski *et al.* [**22**] reported that the interface heat transfer coefficient is strongly dependent on the die pressure and not on the die temperature. Here, the interface heat transfer coefficient shows a modest dependence on the temperature attained during the process. It may be noted that the slight increase in the interface heat transfer coefficient value is for the rubbing speed range 391–558 m/min which falls under the conventional to high-speed machining transition range for AISI 1045 steel [**40**]. It is also important to note that all the estimated values of interface heat transfer coefficient h vary between 100 kW/m^2 °C and 300 kW/m^2 °C. These values fall within the range of assumed values used previously for the simulation of metal machining process (10–100 000 kW/m^2 °C). However, the range is narrower than before. Another important point is that wear of the pin material is not considered in the modelling of rubbing process. This was justifiable because only minute pin wear was recorded (Fig. 7). Significant pin wear may affect the interface heat transfer coefficient value. However, FE modelling of wear mechanisms is a challenging and ongoing task.

10 CONCLUSIONS

Based on the findings from experimental and modelling results, the following conclusions can be drawn:

1. The interface heat transfer coefficient is an important parameter which quantifies the amount of heat transferred to the cutting tool in the FE modelling of mechanical machining processes. The resulting temperature distribution in the cutting tool is, in turn, important for the modelling of tool wear processes. The present practice is to use the interface heat transfer coefficient values estimated from metal-forging process, based on the assumption of perfect contact.
2. Based on the operating ranges of strains, strain rates, and temperatures, the natures of the contact in forging and machining processes are dissimilar. An experimental procedure close to the machining process should be used for the estimation of interface heat transfer coefficient.
3. A new method based on rubbing of a carbide pin of material similar to the cutting tool with AISI 1045 steel as counter material was employed. In addition, an FE model of the rubbing process was developed for the estimation of the interface heat transfer coefficient for a wide range of rubbing speeds.
4. The results show that the estimated interface heat transfer coefficient decreases at low rubbing speeds and then becomes approximately constant for high rubbing speeds. At these low rubbing speeds, the estimated values show a dependence on temperature.
5. All the estimated values of the interface heat transfer coefficient h lie in the range 100–300 kW/m^2 °C. A majority of cutting speeds can be modelled by using an h value equal to 100 kW/m^2 °C. Results suggest that assuming h values lower than 100 kW/m^2 °C or greater than 300 kW/m^2 °C would lead to errors in the estimation of thermal fields and chip morphology. Values of 10 kW/m^2 °C, 500 kW/m^2 °C and 100 000 kW/m^2 °C have been

assumed by some previous researchers without proper justification.

REFERENCES

1 **O'Sullivan, D.** and **Cotterell, M.** Temperature measurement in single point turning. *J Mater. Processing Technol.*, 2001, **118**, 301–308.
2 **Madhusudana, C. V.** *Thermal contact conductance,*, 1996, pp. 1–23 (Springer-Verlag, Berlin).
3 **Yen, Y.-C., Jain, A.,** and **Altan, T.** A finite element analysis of orthogonal machining using different tool edge geometries. *J Mater. Processing Technol.*, 2004, **146**, 72–81.
4 **Yen, Y.-C., Sühner, J., Lilly, B.,** and **Altan, T.** Estimation of tool wear in orthogonal cutting using finite element analysis. *J Mater. Processing Technol.*, 2004, **146**(1), 82–91.
5 **Yen, Y.-C., Jain, A., Chigurupati, P., Wu, W.-T.,** and **Altan, T.** Computer simulation of orthogonal metal cutting using a tool with multiple coatings. *Machining Sci. Technol.*, 2004, **8**(2), 305–326.
6 **Klocke, F., Raedt, H.-W.,** and **Hoppe, S.** 2D-FEM simulation of the orthogonal high speed cutting process. *Machining Sci. Technol.*, 2001, **5**(3), 323–340.
7 **Marusich, T. D.** and **Ortiz, M.** Modelling and simulation of high-speed machining. *Int. J. Numer. Meth. Engng*, 1995, **38**, 3675–3694.
8 **Ozel, T.** The influence of friction models on finite element simulations of machining. *Int. J. Mach. Tools Mf.*, 2006, **46**(6), 518–530.
9 **Xie, L.-J., Schmidt, J., Schmidt, C.,** and **Biesinger, F.** 2D FEM estimate of tool wear in turning operation. *Wear*, 2005, **258**(10), 1479–1490.
10 **Miguelez, H., Zaera, R., Rusine, K. A., Moufki, A.,** and **Molinati, A.** Numerical modelling of orthogonal cutting: Influence of cutting conditions and separation criterion. *J. Physique IV*, 2006, **134**, 417–422.
11 **Coelho, R. T., Ng, E.-G.,** and **Elbestawi, M. A.** Tool wear when turning AISI 4340 with coated PCBN tools using finishing cutting conditions. *Int. J Mach. Tools Mf.*, 2007, **47**, 263–272.
12 **Arrazola, P. J., Villar, A., Ugarte, D.,** and **Marya, S.** Serrated chip prediction in finite element modelling of the chip formation process. *Machining Sci. Technol.*, 2007, **11**(3), 367–390.
13 **Yuen, W. Y. D.** Heat conduction in sliding solids. *Int. J Heat Mass Transfer*, 1988, **31**(3), 637–646.
14 **Cameron, A., Gordon, A. N.,** and **Symm, G. T.** Contact temperatures in rolling/sliding surfaces. *Proc. R. Soci. A*, 1965, **286**(1404), 45–61.
15 **Symm, G. T.** Surface temperature of two rubbing bodies. *J Mechanics Appl. Math.*, 1967, **20**(3), 381–391.
16 **Barber, J. R.** The conduction of heat from sliding solids. *Int. J Heat Mass Transfer*, 1970, **13**, 857–869.
17 **Bos, J.** and **Moes, H.** Frictional heating of tribological contacts. *Trans. ASME J. Tribology*, 1995, **117**, 171–177.
18 **Bauzin, J.-G.** and **Laraqi, N.** Simultaneous estimation of frictional heat flux and two thermal contact parameters for sliding contact. *Numer. Heat Transfer, A*, 2004, **45**, 313–328.
19 **Berry, G. A.** and **Barber, J. R.** The division of frictional heat- a guide to the nature of sliding contact. *Trans. ASME J. Tribology*, 1984, **106**, 405–417.
20 **Lestyan, Z., Varadi, K.,** and **Albers, A.** Contact and thermal analysis of an alumina-steel dry sliding friction pair considering the surface roughness. *Int. J. Mach. Tools Mf.*, 2007, **40**, 982–994.
21 **Semiatin, S. L., Collings, E. W., Wood, V. E.,** and **Altan, T.** Determination of the interface heat transfer coefficient for non isothermal bulk forming process. *Trans. ASME J. Engng Industry*, 1987, **109**, 49–57.
22 **Malinowski, Z., Lenard, J. G.,** and **Davies, M. E.** A study of the heat-transfer coefficient as a function of temperature and pressure. *J. Mater. Processing Technol.*, 1994, **41**, 125–142.
23 **Nshama, W.** and **Jeswiet, J.** Evaluation of temperature and heat transfer conditions at the metal forming interfaces. *Ann. CIRP*, 1995, **44**(1), 201–205.
24 **Burte, P. R., Im, Y. T., Altan, T.,** and **Semiahn, S. L.** Measurements and analysis of the heat transfer and friction during hot forging. *Trans. ASME J. Engng Industry*, 1990, **112**, 332–339.
25 **Goizet, V., Bourouga, B.,** and **Bardon, J. P.** Experimental study of the thermal boundary conditions at the workpiece–die interface during hot forging. In Proceedings of the 11th International Heat Transfer Conference (*IHTC-II*). Kyongju, Republic of Korea, 23–28, August 1998 Vol. 5, pp. 15–20 (Taylor and Francis, London).
26 **Dadras, P.** and **Wells, W. R.** Heat transfer aspects of non-isothermal axisymmetric upset forging. *Trans. ASME J. Engng Industry*, 1984, **106**, 187–195.
27 **Lambert, M. A., Mirmira, S.R.,** and **Fletcher, L. S.** Design graphs for thermal contact conductance of similar and dissimilar light alloys. *J. Thermophysics Heat Transfer*, 2006, **20**(4), 809–816.
28 **Lambert, M. A.** and **Fletcher, L. S.** Thermal contact conductance of non flat, rough, metallic coated metals. *Trans. ASME J. Heat Transfer*, 2002, **124**, 405–412.
29 **Hu, Z. M., Brooks, J. W.,** and **Dean, T. A.** The interfacial heat transfer coefficient in hot die forging of titanium alloy. *Proc. Instn. Mech. Engrs, Part C: J. Mechanical. Engineering. Science*, 1998, **212**(6), 485–496.
30 **Kalpakjian, S.** *Manufacturing processes for engineering materials*, 3rd edition, 1997, (Addison-Wesley/ Longman, Menlo Park, California) 43–102.
31 **Childs, T. H. C.** and **Rowe, G. W.** Physics in metal cutting. *Rep. on Prog. Physics*, 1973, **36**(3), 223–288.
32 **Iqbal, S. A., Mativenga, P. T.,** and **Sheikh, M. A.** Characterization of the machining of AISI 1045 steel over a wide range of cutting speeds – Part 1: Investigation of contact phenomena. *Proc. IMechE, Part B: J. Engineering Manufacture*, 2007, **221**(5), 909–916.
33 **Lancaster, J.** The formation of surface films at the transition between mild and severe metallic wear. *Proc. R. Soc. A*, 1963, **273**, 466–483.
34 **Olsson, M., Söderberg, S., Jacobson, S.,** and **Hogmark, S.** Simulation of cutting tool wear by a modified pin-on-disc test. *Int. J. Mach. Tools Mf.*, 1989, **29**(3), 377–390.
35 **Devillez, A., Lesko, S.,** and **Mozerc, W.** Cutting tool crater wear measurement with white light interferometry. *Wear*, 2004, **256**(1–2), 56–65.

36 Childs, T. H. C., Maekawa, K., Obikawa, T., and **Yamane, Y.** *Metal machining: theory and application*, 2000 (Arnold, London).
37 Abukhshim, N. A., Mativenga, P. T., and **Sheikh, M. A.** Investigation of heat partition in high speed turning of high strength alloy steel. *Int. J. Mach. Tools Mf.*, 2005, **45**(15), 1687–1695.
38 Gecim, B. and **Winer, W. O.** Transient temperatures in the vicinity of an asperity contact. *Trans. ASME J. Tribology*, 1985, **107**, 333–342.
39 Grzesik, W. and **Nieslony, P.** A computational approach to evaluate temperature and heat partition in machining with multilayer coated tools. *Int. J. Mach. Tools Mf.*, 2003, **43**, 1311–1317.
40 Schulz, H. and **Moriwaki, T.** High speed machining. *CIRP Ann.*, 1992, **41**(2), 637–644.

APPENDIX

Notation

C	specific heat capacity (J/kg °C)
h	interface heat transfer coefficient (W/m^2 °C)
h_∞	convective heat transfer coefficient for the surrounding (W/m^2 °C)
H	heat partition coefficient
K	thermal conductivity (W/m °C)
q	heat flux (W/m^2)
ΔT	temperature (°C)
ρ	density (kg/m^3)